INTERNATIONAL JOURNAL OF ADAPTIVE CONTROL AND SIGNAL PROCESSING

Int. J. Adapt. Control Signal Process. 2016; **00**:1–26

Published online in Wiley InterScience (www.interscience.wiley.com). DOI: 10.1002/acs

Fault Estimation in Wind Turbines using a Joint Fault and State Estimation Scheme

Author1, Author2 and Author3

Automatic Control Department, Universitat Politècnica de Catalunya (UPC), Rambla de Sant Nebridi, 11, 08222 Terrassa.

Institute of Control and Computation Engineering, University of Zielona Gora, ul. Podgórna 50, 65-246 Zielona Góra, Poland.

SUMMARY

This paper addresses the problem of fault estimation in wind turbines using a joint fault and state estimation scheme. The scheme assumes a set of possible faults affecting the dynamics of the wind turbine. Then, a joint process fault and state estimation scheme is developed considering that process disturbances and sensor noises are unknown but bounded in an ellipsoid. Two subcases are considered depending of the satisfaction of a rank condition. The proposed scheme is applied to a well-known wind turbine benchmark proposed in a international competition. From the results obtained, a satisfactory fault estimation is achieves against a set of pre-defined fault scenarios. Copyright © 2016 John Wiley & Sons, Ltd.

Received ...

KEY WORDS: Fault estimation, Wind turbine, Unknown but bounded uncertainty, Joint fault and state estimation

*Correspondence to: Damiano Rotondo, Department of Automatic Control (ESAII), Technical University of Catalonia (UPC), Rambla de Sant Nebridi 10, 08222 - Terrassa (Spain). E-mail: damiano.rotondo@upc.edu

1. INTRODUCTION

Nowadays, the generation of electric with wind turbines is a great success all over the world. Every year new wind farm on- and off-shore are being deployed. All forecasts foresee that this evolution will continue in the forthcoming years. However, wind turbines are complex systems that need to be correctly maintained. Moreover, because some of these wind turbines work in difficult meteorological conditions and the accessability to do maintenance is not easy and quite costly (specially those located off-shore), there is a increasing needed of embedding in the wind turbine control systems fault tolerant mechanisms that allow still operating the wind turbine even in case of a fault. In this way, in case of a fault the wind turbine can continue be operated reducing the losses due the stop of energy production and increasing their reliability.

For this reason, the research in Fault Detection and Isolation (FDI) and Fault Tolerant Control (FTC) with application to wind turbines has become a subject of increasing interest in research in both the industry and the academia. In this increased interested, the effort done from the academia, specially from the FDI/FTC community proposing a international competition on FDI and FTC of wind turbines using a realistic wind turbine bechmark, has been remarkable [1, 2]. In [2], a summary of the results obtained in this competition a presented.

Until a few years ago, the application of advanced FDI algorithms in wind turbines were not so widespread. Most to the existing FDI applications were based on some form of signal analysis approach, as e.g. it is proposed in [3]. For a review, on the FDI techniques commonly used in industry and based on signal analysis, the reader is referred to [4]. Morever, there were no FTC applications to wind turbines reported in the literature, the common approach being to monitor the turbine conditions and shut it down in the event a fault were detected [5].

Nowadays, there exist in the literature a large number of FDI approaches for wind turbines. Some of them were compared in the wind turbine FDI competition [2]. Most of these solutions rely on the evaluation of residuals to achieve fault detection and isolation (see, as e.g. [6, 7, 8], among other). However, most of these approaches has been focused on the fault detection and

Prepared using acsauth.cls
DOI: 10.1002/acs

isolation, but not in the fault estimation. Fault estimation is an important step to cover when thinking about the implementation of FTC. The knowledge about the fault size allows to compensate the fault without removing the faulty component (sensor or actuator) and without the need of having hardware redundancy.

In the literature, most of the contributions regarding FTC assume that the fault estimation is already available. To cite just some of these contributions: In[9], a solution to this problem based on the design of passive and active FTC was proposed for a 4.8 MW variable-speed, variable-pitch wind turbine model with a fault in the pitch system. In case of active FTC, a LPV gain-scheduling controller is used that use the fault estimation as the scheduling variable. However, the paper does not provide a mechanism for estimating the fault. The same happens in some other references as: In [10], a fuzzy gain-scheduled active fault-tolerant control of a wind turbine is proposed. In [11], a multiobserver switching control strategy for robust active fuzzy FTC has been proposed for variable-speed wind energy conversion systems subject to sensor faults.

Recently, some authors have realised about the importance of estimating the fault for implementing an active FTC scheme. For example, in [12], an active FTC scheme on adaptive filters obtained via the nonlinear geometric approach is proposed. The controller accommodation scheme exploits the on-line estimate of the actuator fault signal generated by the adaptive filters. In [7], a FTC scheme based on virtual sensors and actuators is proposed where the fault estimation is provided by a parameter estimation scheme. In [13],an active sensor fault tolerant tracking control for offshore wind turbine described via Takagi-Sugeno multiple models is proposed. Due to the dependency of the this strategy on the fault estimation, an observer with the capability to estimate a wide range of time varying fault signals is used. In [14], an observer-based descriptor system AFTC scheme is designed for an offshore wind turbine system using a robust LPV framework, where both the faults and requiered states are estimated. In [15], a Takagi-Sugeno Sliding Mode Observer for actuator fault diagnosis and fault-tolerant control scheme of wind turbines with hydrostatic transmission are presented. A simple compensation approach is implemented by subtracting the reconstructed faults obtained from the faulty inputs.

Prepared using acsauth.cls
DOI: 10.1002/acs

This paper addresses the problem of fault estimation in wind turbines using a joint fault and state estimation scheme. The scheme assumes a set of possible faults affecting the dynamics of the wind turbine. Then, a joint process fault and state estimation scheme is developed assuming that process disturbances and sensor noises are unknown but bounded in an ellipsoid. Two subcases are considered depending of the satisfaction of a rank condition. The proposed scheme is applied to a well-known wind turbine benchmark and tested satisfactorily against a set of pre-defined fault scenarios.

The structure of the paper is as follows: The wind turbine benchmark and considered fault scenarios are presented in Section 2. The proposed approach is presented in Section . Results of the application of the proposed scheme to the considered benchmark are presented presented in Section 4. In Section 5, the conclusions are given and future research directions are suggested.

2. WIND TURBINE BENCHMARK DESCRIPTION

2.1. Introduction

Wind turbines produce electrical energy using the kinetic energy of the wind. The wind turbine considered hereafter is the one proposed in the benchmark described in [2]. This turbine is a variable-speed, pitch-controlled, three-blade horizontal-axis turbine with a full converter coupling. The pressure from the wind on the turbine blades forces the wind turbine rotor to spin around. Then, a rotating shaft converts the kinetic wind energy into mechanical energy. By pitching the blades, or by controlling the rotational speed of the rotor w.r.t. the wind speed, the energy generation can be controlled. A generator, coupled to a converter, performs the conversion from mechanical energy to electrical energy (see [16, 17, 18] for further details about the functioning of wind turbines).

The control system has the objective to follow the power reference or, alternatively, if the wind speed is too low to achieve the desired power reference, to optimize the power production. The controller operates in four operational zones, governed by the mean wind speed within some time window. Zone 1 (turbine at standstill) and zone 4 (high wind speed, for which the energy production

Prepared using acsauth.cls
DOI: 10.1002/acs

of the turbine must be stopped due to safety reasons) are not considered in the benchmark case study, since its aim is to investigate fault detection under normal operations, which correspond to zone 2 (power optimization due to partial load) and zone 3 (constant power production).

2.2. *Wind turbine nonlinear model*

Hereafter, the model of the wind turbine [1] is presented. The overall wind turbine is divided into appropriate sub-models that are modeled separately. The system is driven by the wind speed that affects the aerodynamic properties of the wind turbine, together with the pitch angles of the blades and the speed of the rotor. An aerodynamic torque is transferred from the rotor to the generator through the drive train. Finally, the converter provides the electric power.

Drive Train Model: The drive train model consists of a low-speed shaft and a high-speed shaft having inertias J_r and J_g, and friction coefficients B_r and B_g. The shafts are interconnected by a transmission having a gear ratio N_g and an efficiency η_{dt}, combined with a torsion stiffness K_{dt}, and a torsion damping B_{dt}. It is described by the following three differential equations [9]:

$$\dot{\omega}_r(t) = -\frac{(B_{dt}+B_r)}{J_r}\omega_r(t) + \frac{B_{dt}}{N_g J_r}\omega_g(t) - \frac{K_{dt}}{J_r}\theta_\Delta(t) + \frac{T_r(t)}{J_r} \tag{1}$$

$$\dot{\omega}_g(t) = \frac{\eta_{dt}B_{dt}}{N_g J_g}\omega_r(t) - \left(\frac{\eta_{dt}B_{dt}}{N_g^2 J_g} + \frac{B_g}{J_g}\right)\omega_g(t) + \frac{\eta_{dt}K_{dt}}{N_g J_g}\theta_\Delta(t) - \frac{T_g(t)}{J_g} \tag{2}$$

$$\dot{\theta}_\Delta(t) = \omega_r(t) - \frac{\omega_g(t)}{N_g} \tag{3}$$

where ω_r is the rotor speed, ω_g is the generator speed, θ_Δ is the torsion angle of the drive train, T_r is the aerodynamic torque and T_g is the generator torque. Both the rotor speed ω_r and the generator speed ω_g are measured.

Generator model: The generator torque T_g is controlled by the reference $T_{g,ref}$. The dynamics is approximated by a first order model with time constant τ_g:

$$\dot{T}_g(t) = -\frac{T_g(t)}{\tau_g} + \frac{T_{g,ref}(t)}{\tau_g} \tag{4}$$

Prepared using acsauth.cls
DOI: 10.1002/acs

Pitch system model: The hydraulic pitch system is modeled as a second-order system with input $\beta_{i,ref}$, natural frequency $\omega_{n,i}$ and damping ratio ζ_i [19]:

$$\ddot{\beta}_i(t) = -2\zeta_i\omega_{n,i}\dot{\beta}_i(t) - \omega_{n,i}^2\beta_i(t) + \omega_{n,i}^2\beta_{i,ref}(t) \tag{5}$$

with $i = 1,2,3$. The pitch angles $\beta_i(t)$, $i = 1,2,3$, are measured.

Aerodynamic model: The aerodynamics of the wind turbine is modeled as a torque acting on the blades. This aerodynamics torque $T_r(t)$ can be represented by [20]:

$$T_r(t) = \sum_{i=1}^{3} \frac{\rho\pi R^3 C_q(\lambda(t),\beta_i(t))\, v_w^2(t)}{6} \tag{6}$$

where ρ is the air density, R is the radius of the blades, v_w is the wind speed and C_q is the torque coefficient, which is a function of the pitch angle β_i and the tip speed ratio, defined as:

$$\lambda(t) = \frac{\omega_r(t)R}{v_w(t)} \tag{7}$$

The values of the system parameters used in this paper have been taken from [2] and are resumed in Table I.

Table I. System parameters values

Param.	Value	Param.	Value	Param.	Value
J_r	$55\cdot10^6\,kg\cdot m^2$	η_{dt}	0.97	ω_{n0}	$11.11\,rad/s$
J_g	$390\,kg\cdot m^2$	K_{dt}	$2.7\cdot10^9\,Nm/rad$	ζ_0	0.6
B_r	$7.11\,Nms/rad$	B_{dt}	$775.49\,Nms/rad$	ρ	$1.225\,kg/m^3$
B_{g0}	$45.6\,Nms/rad$	τ_g	$20\cdot10^{-3}\,s$	R	$57.5\,m$
N_g	95	ω_{nf}	$5.73\,rad/s$	ζ_f	0.45
		B_{gf}	$68.4\,Nms/rad$		

2.3. Fault scenarios

In this paper, we consider actuator and process faults affecting different parts of the wind turbine, as defined by [2]. In particular, faults in the pitch system and in the drive train are considered.

Prepared using acsauth.cls
DOI: 10.1002/acs

The hydraulic pitch system can be affected by faults that change the dynamics, due to either a drop in the hydraulic supply system, which can represent a leakage in hose or a blocked pump, or high air content in the oil [2].

In order to model this fault, let us introduce the fault effectiveness parameter $f_i(t)$, such that $f_i(t) = 0$ corresponds to the fault-free i-th pitch system with $\omega_{n,i}^2 = \omega_{n0}^2$, $\zeta_i\omega_{n,i} = \zeta_0\omega_{n0}$, while $f_i(t) = 1$ corresponds to a full fault on the i-th pitch system, such that $\omega_{n,i}^2 = \omega_{nf}^2$, $\zeta_i\omega_{n,i} = \zeta_f\omega_{nf}$ [14]. Hence, both $\omega_{n,i}^2$ and $\zeta_i\omega_{n,i}$ can be described as a function of $f_i(t)$, as follows:

$$\omega_{n,i}^2 = (1 - f_i(t))\,\omega_{n0}^2 + f_i(t)\omega_{nf}^2 \tag{8}$$

$$\zeta_i\omega_{n,i} = (1 - f_i(t))\,\zeta_0\omega_{n0} + f_i(t)\zeta_f\omega_{nf} \tag{9}$$

It is simple to check that (5), together with (8)-(9), and taking into account the available measurements, can be rewritten in state space form as [14]:

$$\begin{bmatrix} \dot{\beta}_i(t) \\ \ddot{\beta}_i(t) \end{bmatrix} = \begin{bmatrix} 0 & 1 \\ -\omega_{n0}^2 & -2\zeta_0\omega_{n0} \end{bmatrix} \begin{bmatrix} \beta_i(t) \\ \dot{\beta}_i(t) \end{bmatrix} + \begin{bmatrix} 0 \\ \omega_{n0}^2 \end{bmatrix} \beta_{i,ref}(t) + \begin{bmatrix} 0 \\ 1 \end{bmatrix} z_{\beta i}(t) \tag{10}$$

$$y_{\beta_i}(t) = \begin{bmatrix} 1 & 0 \end{bmatrix} \begin{bmatrix} \beta_i(t) \\ \dot{\beta}_i(t) \end{bmatrix} \tag{11}$$

with:

$$z_{\beta i}(t) = f_i(t) \left[\left(\omega_{n0}^2 - \omega_{nf}^2\right) \beta_i(t) + 2\left(\zeta_0\omega_{n0} - \zeta_f\omega_{nf}\right) \dot{\beta}_i(t) + \left(\omega_{nf}^2 - \omega_{n0}^2\right) \beta_{i,ref}(t) \right] \tag{12}$$

On the other hand, the fault in the drive train consists in a change of the high-speed shaft friction coefficient B_g, which is modeled by replacing B_{g0} by a lower value B_{gf}. Similarly to the pitch system case, let us introduce the parameter $f_g(t)$ such that:

$$B_g = (1 - f_g(t))\,B_{g0} + f_g(t)B_{gf} \tag{13}$$

Prepared using acsauth.cls
DOI: 10.1002/acs

Hence, taking into account the available measurements, (1)-(3) can be rewritten in state space form as:

$$\begin{bmatrix} \dot{\omega}_r(t) \\ \dot{\omega}_g(t) \\ \dot{\theta}_\Delta(t) \end{bmatrix} = \begin{bmatrix} -\frac{B_{dt}+B_r}{J_r} & \frac{B_{dt}}{N_g J_r} & -\frac{K_{dt}}{J_r} \\ \frac{\eta_{dt}B_{dt}}{N_g J_g} & -\left(\frac{\eta_{dt}B_{dt}}{N_g^2 J_g}+\frac{B_{g0}}{J_g}\right) & \frac{\eta_{dt}K_{dt}}{N_g J_g} \\ 1 & -\frac{1}{N_g} & 0 \end{bmatrix} \begin{bmatrix} \omega_r(t) \\ \omega_g(t) \\ \theta_\Delta(t) \end{bmatrix} + \begin{bmatrix} \frac{1}{J_r} & 0 \\ 0 & -\frac{1}{J_g} \\ 0 & 0 \end{bmatrix} \begin{bmatrix} T_r(t) \\ T_g(t) \end{bmatrix} + \begin{bmatrix} 0 \\ 1 \\ 0 \end{bmatrix} z_g(t) \tag{14}$$

$$y_{dt}(t) = \begin{bmatrix} 1 & 0 & 0 \\ 0 & 1 & 0 \end{bmatrix} \begin{bmatrix} \omega_r(t) \\ \omega_g(t) \end{bmatrix} \tag{15}$$

with:

$$z_g(t) = \frac{f_g(t)\left(B_{g0}-B_{gf}\right)}{J_g}\omega_g(t) \tag{16}$$

3. JOINT STATE AND FAULT ESTIMATION

Let us consider a discrete-time system described by the following:

$$x(k+1) = Ax(k) + Bu(k) + Dz(k) + W_1 w_1(k), \tag{17}$$

$$y(k) = Cx(k) + W_2 w_2(k), \tag{18}$$

where $x \in \mathbb{R}^n$, $y \in \mathbb{R}^m$, $u \in \mathbb{R}^r$, $z \in \mathbb{R}^q$ are the state, output, input and process fault vectors, respectively. The matrix $D \in \mathbb{R}^{n\times q}$, with $rank(D) = q < n$, is denoted as *fault distribution matrix*, and describes the way in which the faults $z(k)$ affects the system. Moreover, W_1 and W_2 denote the distribution matrices for the exogenous disturbances/noises w_1 and w_2, which affect the state and the output, respectively. Notice that both (10)-(11) and (14)-(15) can be rewritten in the form (17)-(18) through discretization, e.g. using the Euler method, by considering the presence of exogenous disturbances.

Prepared using acsauth.cls
DOI: 10.1002/acs

The problem is to design an estimator that is able to estimate simultaneously the state and the process fault. In the following, the proposed estimator will be called *Process Fault Estimator* (PFE). Notice that the joint estimation of state and fault variables x and z allows also estimating the fault effectiveness parameters. In fact, by using the estimates $\hat{\beta}_i(k)$, $\hat{\bar{\beta}}_i(k)$ and $\hat{z}_{\beta_i}(k)$, the estimation $\hat{f}_i(k)$ can be extracted from (12) using parameter estimation techniques, such as least squares methods [21]. In the same way, by using the estimates $\hat{\omega}_g(k)$ and $\hat{z}_g(k)$, a value $\hat{f}_g(k)$ can be extracted from (16).

For the purpose of further developments, the following assumptions are considered regarding the effect of faults, disturbances and noises:

Assumption 1:

$$\varepsilon(k) \triangleq z(k+1) - z(k) \in \mathscr{E}_\varepsilon = \{\varepsilon : \varepsilon^T Q_\varepsilon \varepsilon \leq 1\}, \quad Q_\varepsilon \succ 0. \tag{19}$$

Assumption 2:

$$\begin{aligned} w_1(k) &\in \mathscr{E}_{w_1} = \{w_1 : w_1^T Q_{w_1} w_1 \leq 1\}, \quad Q_{w_1} \succ 0, \\ w_2(k) &\in \mathscr{E}_{w_2} = \{w_2 : w_2^T Q_{w_2} w_2 \leq 1\}, \quad Q_{w_2} \succ 0. \end{aligned} \tag{20}$$

Assumption 1 is required for the subsequent fault estimation algorithm. It has well defined roots as all real faults and states are bounded, which means that $z(k)$ is bounded as well. Similarly, *Assumption 2* states that the external disturbances are unknown but bounded.

In the remaining of this section, two different estimators are proposed to solve the above-defined estimation problem, depending on whether or not the following condition holds true:

$$rank(CD) = rank(D) = q \tag{21}$$

Notice that the rank condition (21) does not hold for the pitch subsystem obtained from (10)-(11). On the other hand, it holds true for the drive train subsystem obtained from (14)-(15).

Prepared using acsauth.cls
DOI: 10.1002/acs

3.1. Case 1: $rank(CD) \neq rank(D)$

For this case, the following estimator is proposed:

$$\hat{x}(k+1) = A\hat{x}(k) + Bu(k) + D\hat{z}(k) + K\left(y(k) - C\hat{x}(k)\right) \tag{22}$$

$$\hat{z}(k+1) = \hat{z}(k) + L\left(y(k) - C\hat{x}(k)\right) \tag{23}$$

where $K \in \mathbb{R}^{n\times m}$ and $L \in \mathbb{R}^{q\times m}$ are gains to be designed.

From (17)-(18), the evolution of the state estimation error $e(k) \triangleq x(k) - \hat{x}(k)$ is described by:

$$e(k+1) = (A - KC)\, e(k) + De_z(k) + W_1 w_1(k) - KW_2 w_2(k) \tag{24}$$

where $e_z(k) \triangleq z(k) - \hat{z}(k)$.

Subsequently, the dynamics of the fault estimation error $e_z(k)$ is given by:

$$\begin{aligned} e_z(k+1) &= z(k+1) + z(k) - z(k) - \hat{z}(k+1) = \varepsilon(k) + z(k) - \hat{z}(k+1) \\ &= \varepsilon(k) + z(k) - \hat{z}(k) - LCx(k) - LW_2 w_2(k) + LC\hat{x}(k) \\ &= \varepsilon(k) + e_z(k) - LCe(k) - LW_2 w_2(k), \end{aligned} \tag{25}$$

where $\varepsilon(k)$ is defined as in (19).

By introducing the following vectors:

$$\bar{e}(k) = \left[e(k)^T, e_z(k)^T\right]^T, \tag{26}$$

$$v(k) = \left[w_1(k)^T, w_2(k)^T, \varepsilon(k)^T\right]^T, \tag{27}$$

the state and fault estimation error dynamics are given by:

$$\bar{e}(k+1) = \begin{bmatrix} A - KC & D \\ -LC & I \end{bmatrix} \bar{e}(k) + \begin{bmatrix} W_1 & -KW_2 & 0 \\ 0 & -LW_2 & I \end{bmatrix} v(k). \tag{28}$$

Prepared using acsauth.cls
DOI: 10.1002/acs

which can be described in an equivalent form:

$$\bar{e}(k+1) = X\bar{e}(k) + Zv(k), \tag{29}$$

where:

$$X = \bar{A} - \bar{K}\bar{C} = \begin{bmatrix} A & D \\ 0 & I \end{bmatrix} - \begin{bmatrix} K \\ L \end{bmatrix} \begin{bmatrix} C & 0 \end{bmatrix}, \tag{30}$$

$$Z = \bar{W} - \bar{K}\bar{V} = \begin{bmatrix} W_1 & 0 & 0 \\ 0 & 0 & I \end{bmatrix} - \begin{bmatrix} K \\ L \end{bmatrix} \begin{bmatrix} 0 & W_2 & 0 \end{bmatrix}. \tag{31}$$

The ellipsoidal set including $v(k)$ can be described by:

$$\mathscr{E}_v = \{v : v^T Q_v v \leq 1\}, \tag{32}$$

with

$$Q_v = \frac{1}{3}\text{diag}\left(Q_{w_1}, Q_{w_2}, Q_\varepsilon\right). \tag{33}$$

Notice that, if $v(k) = 0$, then the usual Lyapunov approach can be used to prove the asymptotic convergence of $\bar{e}(k)$. However, if $v(k) \neq 0$ then such approach cannot be applied directly. Thus, for the purpose of further deliberations, the so-called quadratic boundedness (QB) [22, 23, 24] approach is used. To do so, let us define the Lyapunov function:

$$V(k) = \bar{e}(k)^T P \bar{e}(k), \tag{34}$$

with $P \succ 0$, and let us remind the following definitions [22, 23, 24]:

***Definition** 1*

The system (29) is strictly quadratically bounded for all allowable $v \in \mathscr{E}_v$, implying $\bar{e}(k)^T P \bar{e}(k) > 1$ if $\bar{e}(k+1)^T P \bar{e}(k+1) < \bar{e}(k)^T P \bar{e}(k)$ for any $v(k) \in \mathscr{E}_v$.

Prepared using acsauth.cls
DOI: 10.1002/acs

It should be highlighted that the strict quadratic boundedness of (29) ensures that $V(k+1) < V(k)$ for any $v \in \mathscr{E}_v$ when $V(k) > 1$.

***Definition** 2*

A set $\mathscr{E}$ is a positively invariant set for (29) for all $v \in \mathscr{E}_v$ if $\bar{e}(k) \in \mathscr{E}$ implying $\bar{e}(k+1) \in \mathscr{E}$ for any $v(k) \in \mathscr{E}_v$

Based on these definitions and the results presented in [22], the following lemma can be formulated for (29):

***Lemma** 1*

The following statements are equivalent [22, 23, 24]:

1. The system (29) is strictly quadratically bounded for all $v \in \mathscr{E}_v$.
2. The ellipsoid

$$\mathscr{E} = \{\bar{e} : \bar{e}^T P \bar{e} \leq 1\}, \tag{35}$$

   is an invariant set for (29) for any $v \in \mathscr{E}_v$.
3. There exists a scalar $\alpha \in (0,1)$ such that:

$$\begin{bmatrix} X^T PX - P + \alpha P & X^T PZ \\ Z^T PX & Z^T PZ - \alpha Q_v \end{bmatrix} \preceq 0. \tag{36}$$

To provide the final design procedure, the following theorem is proposed:

***Theorem** 1*

The system (29) is strictly quadratically bounded for all $v \in \mathscr{E}_v$ if there exist matrices $P \succ 0$, U and a scalar $\alpha \in (0,1)$, such that the following inequality is satisfied:

$$\begin{bmatrix} -P + \alpha P & 0 & \bar{A}^T P - \bar{C}^T U^T \\ 0 & -\alpha Q_v & \bar{W}^T P - \bar{V}^T U^T \\ P\bar{A} - U\bar{C} & P\bar{W} - U\bar{V} & -P \end{bmatrix} \preceq 0. \tag{37}$$

Prepared using acsauth.cls
DOI: 10.1002/acs

Proof

Inequality (36) can be rewritten into the following form:

$$\begin{bmatrix} X^T \\ Z^T \end{bmatrix} P \begin{bmatrix} X & Z \end{bmatrix} + \begin{bmatrix} -P+\alpha P & 0 \\ 0 & -\alpha Q_v \end{bmatrix} \preceq 0. \tag{38}$$

Then, using the Schur complement and multiplying left and right side by $\mathrm{diag}(I,I,P)$ gives

$$\begin{bmatrix} -P+\alpha P & 0 & X^T P \\ 0 & -\alpha Q_v & Z^T P \\ PX & PZ & -P \end{bmatrix} \preceq 0. \tag{39}$$

Substituting

$$PX = P\bar{A} - P\bar{K}\bar{C} = P\bar{A} - U\bar{C}, \tag{40}$$

$$PZ = P\bar{W} - P\bar{K}\bar{V} = P\bar{W} - UV, \tag{41}$$

and introducing (40) and (41) into (39) completes the proof. □

Finally, the design procedure boils down to solve (37) and then calculating

$$\bar{K} = \begin{bmatrix} K \\ L \end{bmatrix} = P^{-1}U. \tag{42}$$

A complete design procedure of the PFE is depicted in Fig. 1.

3.2. Case 2: rank(CD) = rank(D)

In this case, by combining (17) and (18), the following is obtained:

$$CDz(k) = y(k+) - CAx(k) - CBu(k) - CW_1 w_1(k) - W_2 w_2(k+1) \tag{43}$$

Prepared using acsauth.cls
DOI: 10.1002/acs

which is an identity, since for given vectors $z(k)$, $x(k)$, $u(k)$, $w_1(k)$, $w_2(k)$, the value of the vector $y(k+1)$ cannot be arbitrary, but is determined by (17) and (18). It follows that if $z(k)$ is considered unknown, the linear system of equations resulting from (43) would admit a solution (i.e. the actual value of $z(k)$), which could be obtained as follows:

$$z(k) = H\left[y(k+1) - CAx(k) - CBu(k) - CW_1w_1(k) - W_2w_2(k+1)\right] \tag{44}$$

where H denotes the Moore-Penrose pseudoinverse of CD.

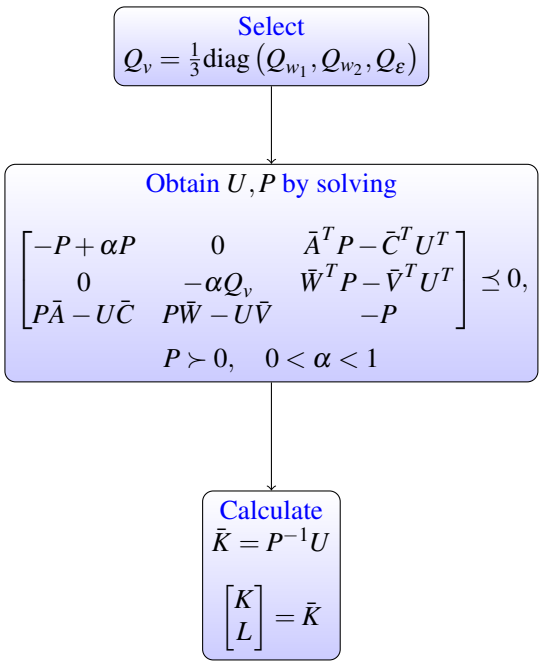

Figure 1. PFE design procedure

Due to the rank condition (21), (44) is the unique solution of the linear system obtained from (43). Moreover, H can be calculated easily as follows:

$$H = (CD)^{\dagger} = \left[(CD)^T CD\right]^{-1} (CD)^T \tag{45}$$

where † denotes the Moore-Penrose pseudoinverse.

Prepared using acsauth.cls
DOI: 10.1002/acs

By substituting (44) into (17), it can be shown that:

$$x(k+1) = \bar{A}x(k) + \bar{B}u(k) + \bar{H}y(k+1) + \bar{W}_1 w_1(k) + \bar{W}_2 w_2(k+1) \tag{46}$$

where:

$$\bar{A} = (I - DHC)A \tag{47}$$

$$\bar{B} = (I - DHC)B \tag{48}$$

$$\bar{H} = DH \tag{49}$$

$$\bar{W}_1 = (I - DHC)W_1 \tag{50}$$

$$\bar{W}_2 = -DHW_2 \tag{51}$$

Based on (44) and (46), the following estimator is proposed:

$$\hat{x}(k+1) = \bar{A}\hat{x}(k) + \bar{B}u(k) + \bar{H}y(k+1) + K(y(k) - C\hat{x}(k)) \tag{52}$$

$$\hat{z}(k) = H(y(k+1) - CA\hat{x}(k) - CBu(k)) \tag{53}$$

where $K \in \mathbb{R}^{n\times m}$ is the gain to be designed.

Then, the associated state estimation error is given by:

$$e(k+1) = \left(\bar{A} - KC\right)e(k) + \bar{W}_1 w_1(k) - KW_2 w_2(k) + \bar{W}_2 w_2(k+1) \tag{54}$$

while the fault estimation error is described by:

$$e_z(k) = -HCAe(k) - HCW_1 w_1(k) - HCW_2 w_2(k+1) \tag{55}$$

From (54)-(55), it can be seen that the dynamics of $e(k)$ does not depend on $e_z(k)$, while at the same time there exists a static relationship between $e(k)$, $w_1(k)$, $w_2(k+1)$ and $e_z(k)$.

Prepared using acsauth.cls
DOI: 10.1002/acs

For this reason, in order to design the gain K, the QB-based procedure described previously can be applied, starting from (29), but using:

$$\bar{e}(k) = e(k) \tag{56}$$

$$v(k) = \left[w_1(k)^T, w_2(k)^T, w_2(k+1)^T\right]^T \tag{57}$$

$$X = \bar{A} - KC \tag{58}$$

$$Z = \begin{bmatrix} \bar{W}_1 & 0 & \bar{W}_2 \end{bmatrix} - K \begin{bmatrix} 0 & W_2 & 0 \end{bmatrix} \tag{59}$$

$$Q_v = \frac{1}{3} diag\left(Q_{w_1}, Q_{w_2}, Q_{w_2}\right) \tag{60}$$

4. APPLICATION TO THE WIND TURBINE CASE STUDY

4.1. Fault scenario 1: faults in the pitch subsystem

First of all, let us evaluate the effectiveness of the PFE described in Section 3.1, i.e. for the case where (21) does not hold, by considering faults affecting the pitch system, as described in Section 2.3.

The design procedure described in Section 3.1 has been applied to the discrete-time model obtained from (10)-(11) using an Euler discretization with sampling time $T_s = 0.01\,s$.

The exogenous disturbance distribution matrices are considered as follows:

$$W_1 = \begin{bmatrix} 1 \\ \\ 0 \end{bmatrix} \qquad\qquad W_2 = 1$$

while the matrices Q_ε, Q_{w_1} and Q_{w_2} are:

$$Q_{w_1} = 1000 \quad Q_{w_2} = 10^6 \quad Q_\varepsilon = 100$$

Prepared using acsauth.cls
DOI: 10.1002/acs

Theorem 1 has been applied for designing the gains K, L, with a value $\alpha = 0.1$, obtaining:

$$P = 10^3 \begin{bmatrix} 1.8242 & -0.0397 & -0.0052 \\ -0.0397 & 0.0829 & -0.0049 \\ -0.0052 & -0.0049 & 0.0004 \end{bmatrix}$$

$$K = \begin{bmatrix} 0.7843 \\ 4.7511 \end{bmatrix} \qquad L = 88.2718$$

In order to assess the performance of this observer, the following evolution of the signal $f_1(t)$ (fault in the first pitch system) has been considered:

$$f_1(t) = \begin{cases} 0 & t \leq 2900\,s \\ 1 & 2900\,s < t \leq 3000\,s \\ 0 & 3000\,s < t \leq 3500\,s \\ \frac{t-3500}{30} & 3500\,s < t \leq 3530\,s \\ 1 & 3530\,s < t \leq 3570\,s \\ \frac{3600-t}{30} & 3570\,s < t \leq 3600\,s \\ 0 & 3600\,s < t \leq 4100\,s \\ 1 & 4100\,s < t \leq 4300\,s \\ 0 & else \end{cases} \tag{61}$$

which contains both abrupt and incipient faults.

The results shown hereafter refer to a simulation that lasts $4400\,s$, where the input for the first pitch system $\beta_{ref,1}(t)$ is as depicted in Fig. 2.

Fig. 3 shows the evolution of the state variables $\beta_1(t)$ and $\dot{\beta}_1(t)$, and their estimation using the designed observer. On the other hand, Fig. 4 shows the estimation errors for both the state variables $\beta_1(t)$ and $\dot{\beta}_1(t)$. It can be seen that the designed observer is able to estimate correctly the state, although its effectiveness is affected by the presence of faults.

Prepared using acsauth.cls
DOI: 10.1002/acs

Fig. 6 compares the fault signal $z_{\beta_1}(t)$ with its estimation. It can be seen that $\hat{z}_{\beta_1}$ is affected by the presence of exogenous disturbances even when no fault acts on the system. This motivates the introduction of a threshold-based filtering which returns $\hat{z}_{\beta_1,filt.}$, as follows:

$$\hat{z}_{\beta_1,filt.}(k) = \begin{cases} \hat{z}_{\beta_1} & if\ \hat{z}_{\beta_1} \geq 0.6 \\ 0 & else \end{cases}$$

Then, recursive least squares with forgetting factor 0.997 are applied taking into account (12), obtaining the estimation of the fault effectiveness parameter $\hat{f}_1$, which is shown in Figs. 6-7. Taking into account the presence of external disturbances, noise, and discretization errors, the obtained estimation is considered to be satisfactorily accurate.

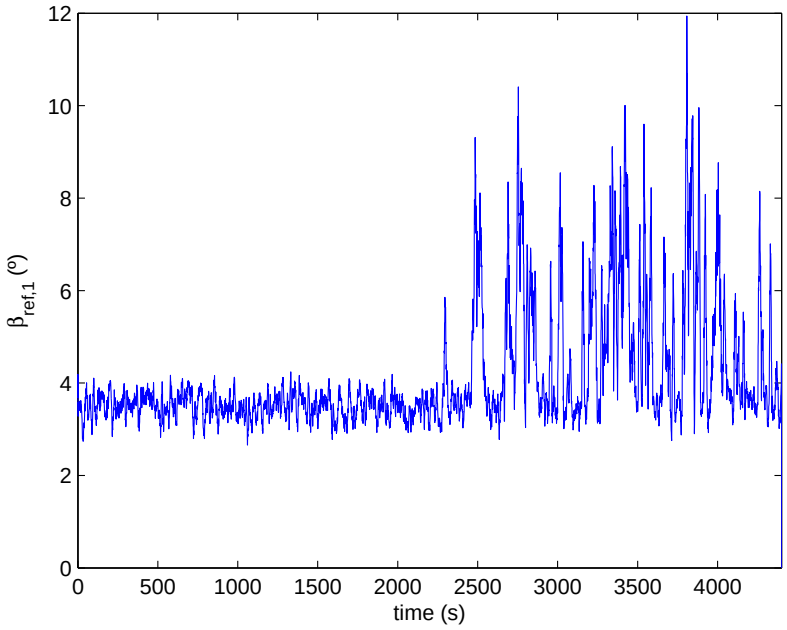

Figure 2. Reference for the pitch system 1: $\beta_{1,ref}$.

4.2. Fault scenario 2: faults in the drive train subsystem

Let us now evaluate the effectiveness of the PFE described in Section 3.2, i.e. for the case where (21) holds, by considering faults affecting the drive train subsystem, as described in Section 2.3.

Prepared using acsauth.cls
DOI: 10.1002/acs

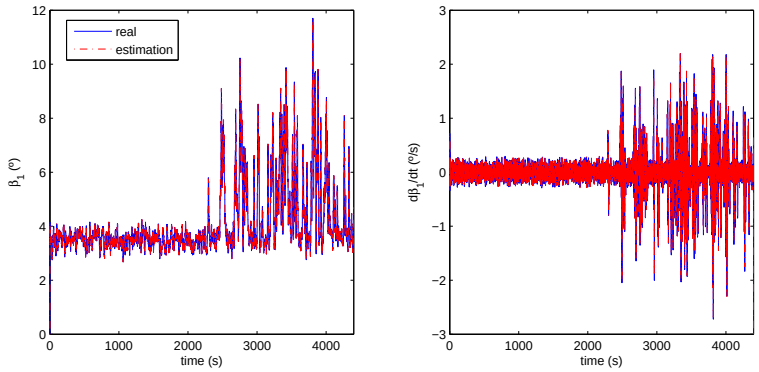

Figure 3. Pitch system 1: state variables β_1 and $\dot{\beta}_1$ (real vs. estimation).

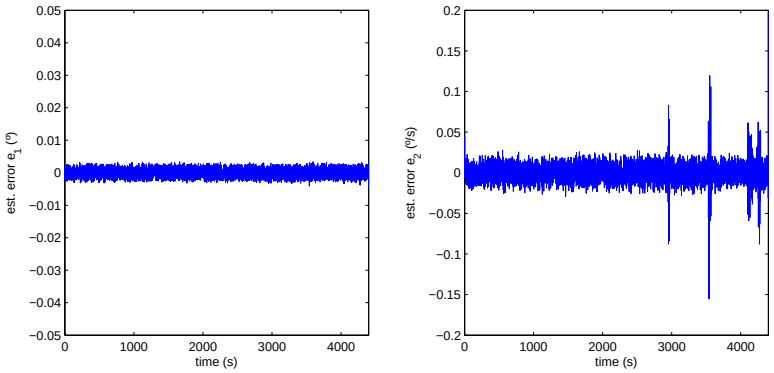

Figure 4. Estimation errors $e_1 = \beta_1 - \hat{\beta}_1$, $e_2 = \dot{\beta}_1 - \hat{\dot{\beta}}_1$.

The design procedure described in Section 3.2 has been applied to the discrete-time model obtained from (14)-(15) using an Euler discretization with sampling time $T_s = 0.01\,s$.

The exogenous disturbance matrices are considered as follows:

$$W_1 = \begin{bmatrix} 1 & 0 \\ 0 & 1 \\ 0 & 0 \end{bmatrix} \qquad W_2 = \begin{bmatrix} 1 & 0 \\ 0 & 1 \end{bmatrix}$$

while the matrices Q_{w_1} and Q_{w_2} are:

$$Q_{w_1} = \begin{bmatrix} 10^8 & 0 \\ 0 & 5 \cdot 10^8 \end{bmatrix} \qquad Q_{w_2} = \begin{bmatrix} 10^6 & 0 \\ 0 & 10^6 \end{bmatrix}$$

Prepared using acsauth.cls
DOI: 10.1002/acs

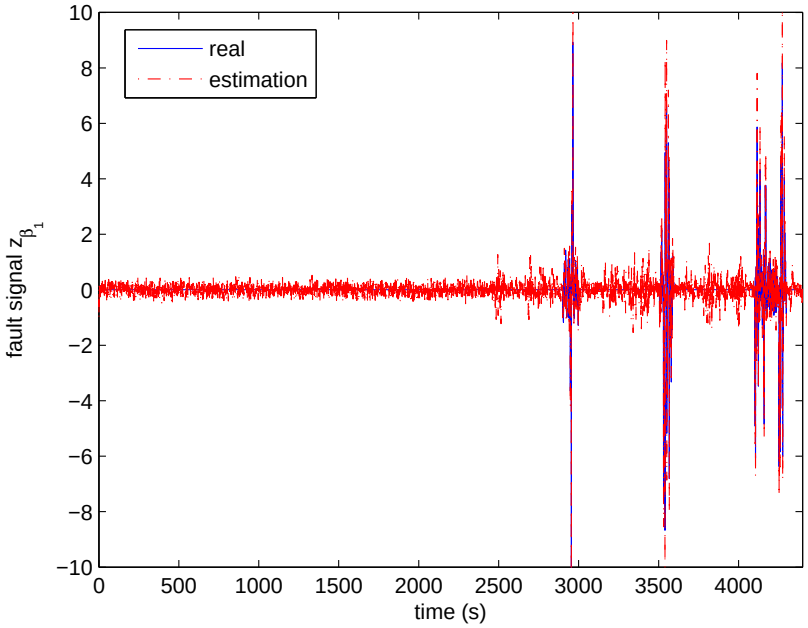

Figure 5. Fault signal z_{β_1} (real vs. estimation).

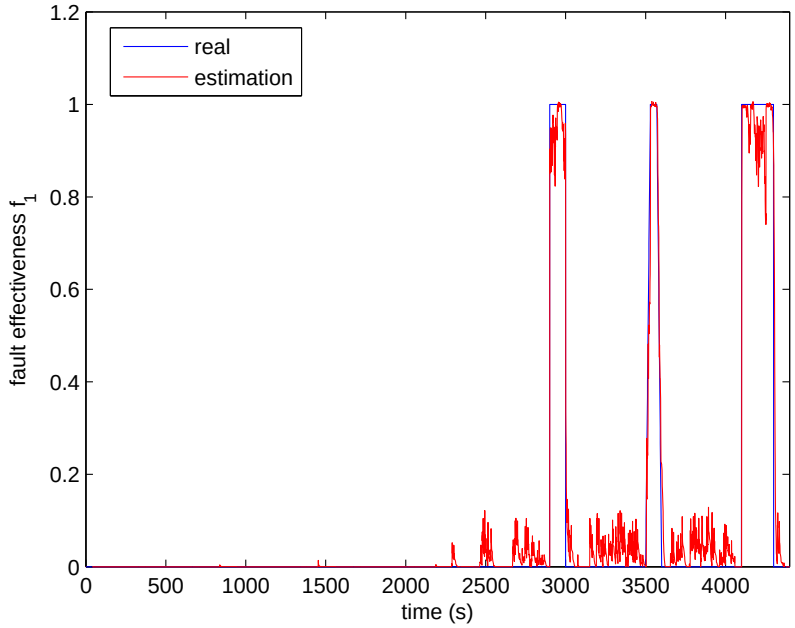

Figure 6. Fault effectiveness f_1 (real vs. estimation).

Theorem 1 has been applied for designing the gain K, with a value $\alpha = 0.1$, obtaining:

Prepared using acsauth.cls
DOI: 10.1002/acs

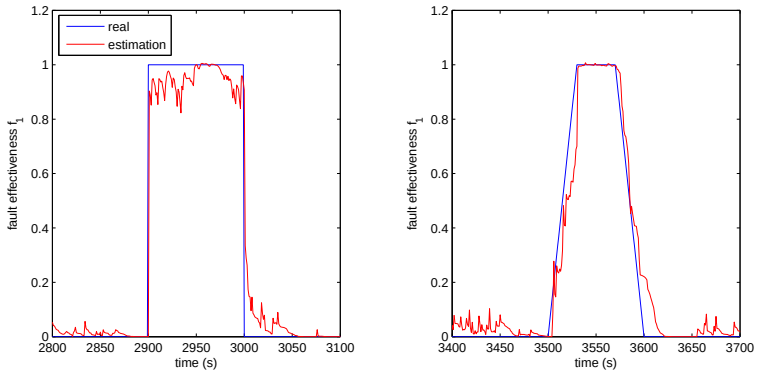

Figure 7. Fault effectiveness f_1 (real vs. estimation, zoom).

$$P = 10^4 \cdot \begin{bmatrix} 0.3364 & 0.3916 & 0.1799 \\ 0.3916 & 3.1667 & 0.1778 \\ 0.1799 & 0.1778 & 0.4687 \end{bmatrix} \qquad K = \begin{bmatrix} 1.1843 & 0.9086 \\ -0.0036 & -0.0485 \\ -0.4081 & -0.3402 \end{bmatrix}$$

In order to assess the performance of this observer, an evolution of the signal $f_g(t)$ similar to the one of $f_1(t)$ provided in (61) has been considered.

The results shown hereafter refer to a simulation that lasts $4400\,s$, where the inputs $T_r(t)$ and $T_g(t)$ are as shown in Fig. 8.

Fig. 9 shows the evolution of the state variables $\omega_r(t)$, $\omega_g(t)$, $\theta_\Delta(t)$ and their estimation. The effectiveness of the designed observer is confirmed by the state estimation errors, which are plotted in Fig. 10.

Fig. 11 compares the fault signal $z_g(t)$ with its estimation. In this case, the distinction between the effect of the exogenous disturbances and the effect of the fault is not strong enough to motivate the introduction of a threshold-based filtering.

Nevertheless, when recursive least squares with forgetting factor 0.997 are applied taking into account (16), a satisfactory estimation of the fault effectiveness parameter f_g is obtained, as shown in Figs. 12-13.

Prepared using acsauth.cls
DOI: 10.1002/acs

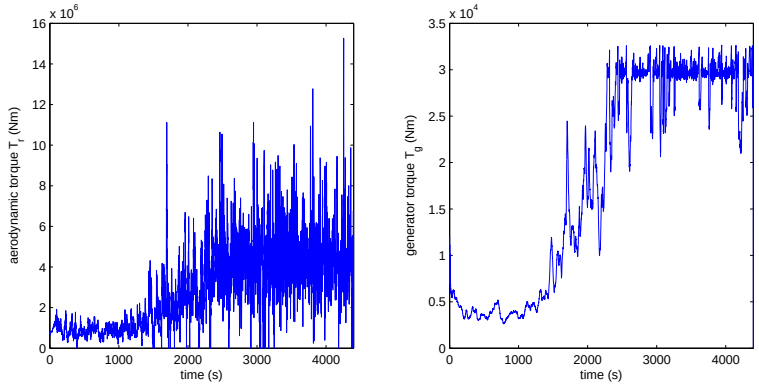

Figure 8. Inputs for the drive train subsystem: T_r and T_g.

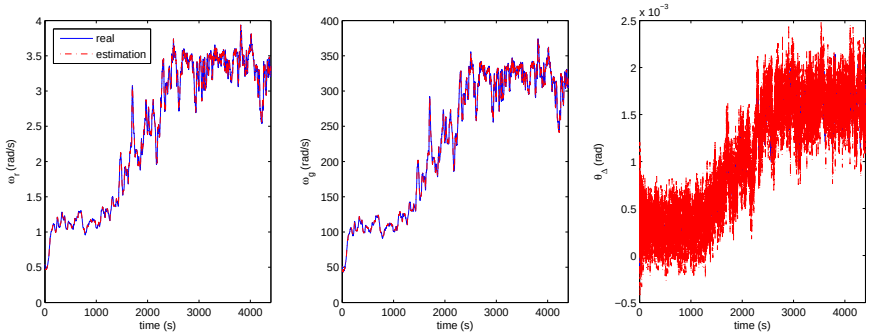

Figure 9. Drive train subsystem: state variables ω_r, ω_g and θ_Δ (real vs. estimation).

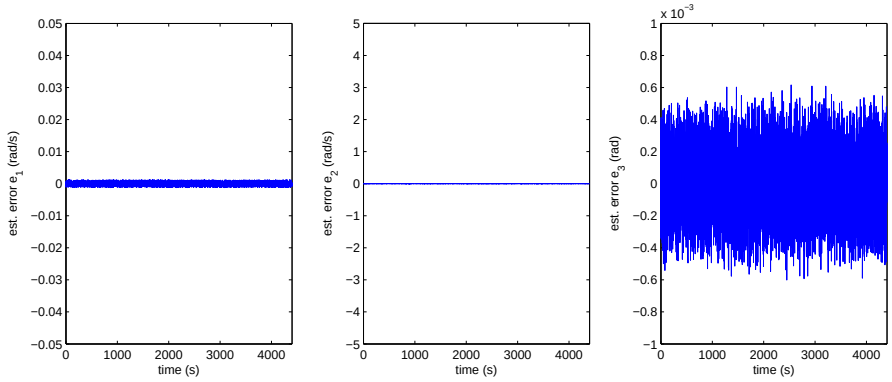

Figure 10. Estimation errors $e_1 = \omega_r - \hat{\omega}_r$, $e_2 = \omega_g - \hat{\omega}_g$ and $e_3 = \theta_\Delta - \hat{\theta}_\Delta$.

5. CONCLUSIONS

This paper has presented a joint fault and state estimation scheme and its application to the fault estimation in a benchmark wind turbine. The scheme assumes a set of possible faults affecting the dynamics of the wind turbine. From the model of the system including the considered faults, a

Prepared using acsauth.cls
DOI: 10.1002/acs

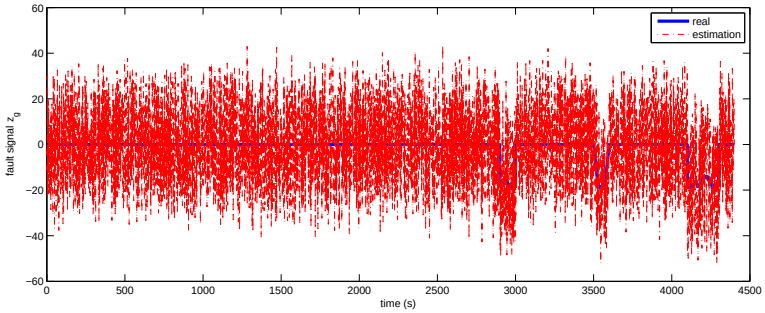

Figure 11. Fault signal z_g (real vs. estimation).

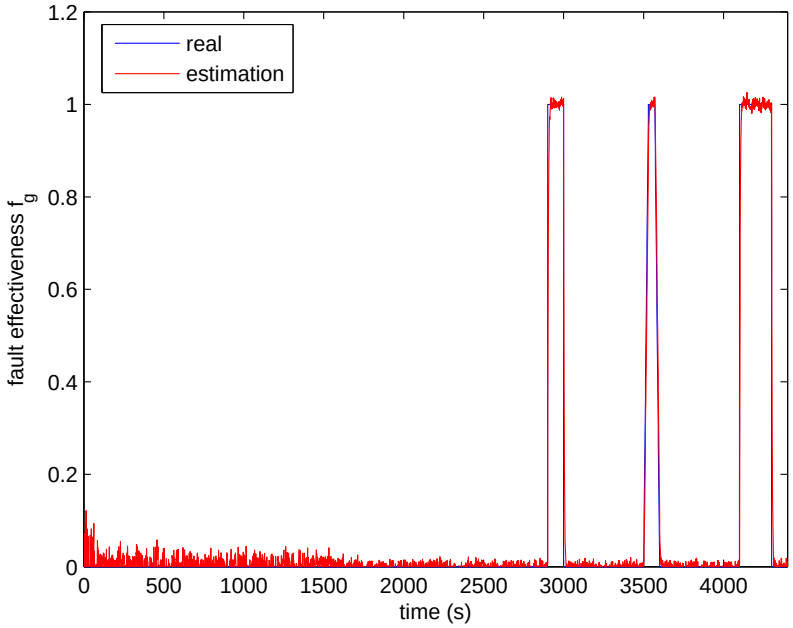

Figure 12. Fault effectiveness f_g (real vs. estimation).

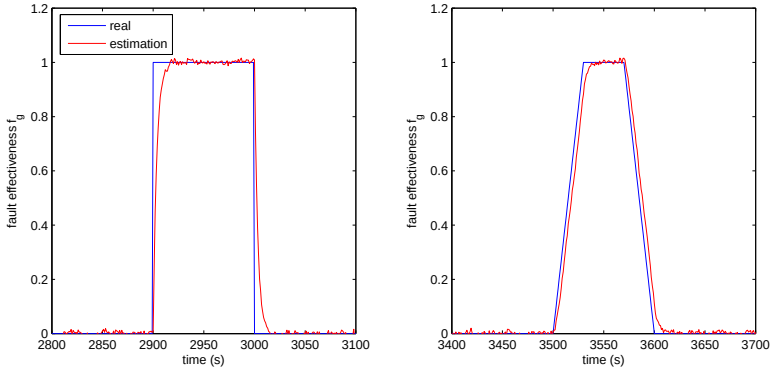

Figure 13. Fault effectiveness f_g (real vs. estimation, zoom).

Prepared using acsauth.cls
DOI: 10.1002/acs

joint process fault and state estimation scheme has been developed. The proposes scheme assumes that process disturbances and sensor noises are bounded in an ellipsoid. The proposed scheme has been applied to a well-known wind turbine benchmark. From the results obtained in simulation considering a set of pre-defined fault scenarios, it has been assessed the satisfactory performance of the proposed scheme for fault estimation. As a further research, it is planned to extend the proposed scheme to non-linear systems via the LPV or TS approach. Moreover, it is planned to integrate this joint fault and state estimation scheme with a fault-tolerant control scheme that relies on the developed LPV/TS extended approach.

6. ACKNOWLEDGEMENTS*

REFERENCES

[1] Odgaard PF, Stoustrup J, Kinnaert M. Fault tolerant control of wind turbines - a benchmark model. *Proceedings of the 7th IFAC symposium on fault detection, supervision and safety of technical processes (SAFEPROCESS09)*, 2009; 155–160.

[2] Odgaard PF, Johnson KE. Wind turbine fault detection and fault tolerant control - an enhanced benchmark challenge. *2013 American Control Conference*, 2013; 4447–4452.

[3] Development, implementation, and testing of fault detection strategies on the national wind technology center controls advanced research turbines. *Mechatronics* 2011; **21**(4):728 – 736.

[4] Hameed Z, Hong Y, Cho Y, Ahn S, Song C. Condition monitoring and fault detection of wind turbines and related algorithms: A review. *Renewable and Sustainable Energy Reviews* 2009; **13**(1):1–39.

[5] Esbensen T, Sloth C. Fault diagnosis and fault-tolerant control of wind turbines. Master's Thesis, Aalborg University 2009.

Prepared using acsauth.cls
DOI: 10.1002/acs

[6] Observer-based {FDI} schemes for wind turbine benchmark. *Proceedings of 18th {IFAC} IFAC World Congress, Milano, Italy* 2011; **44**(1):7073 – 7078.

[7] {FDI} and {FTC} of wind turbines using the interval observer approach and virtual actuators/sensors. *Control Engineering Practice* 2014; **24**:138 – 155.

[8] Data-driven fault detection and isolation scheme for a wind turbine benchmark. *Renewable Energy* 2016; **87, Part 1**:634 – 645.

[9] Sloth C, Esbensen T, Stoustrup J. Robust and fault-tolerant linear parameter-varying control of wind turbines. *Mechatronics* 2011; **21**:645–659.

[10] Fuzzy gain-scheduled active fault-tolerant control of a wind turbine. *Journal of the Franklin Institute* 2014; **351**(7):3677 – 3706.

[11] Robust fuzzy scheduler fault tolerant control of wind energy systems subject to sensor and actuator faults. *International Journal of Electrical Power and Energy Systems* 2014; **55**:402–419.

[12] Simani S, Castaldi P. Active actuator fault-tolerant control of a wind turbine benchmark model. *International Journal of Robust and Nonlinear Control* 2014; **24**(8-9):1283–1303.

[13] Active sensor fault tolerant output feedback tracking control for wind turbine systems via t-s model. *Engineering Applications of Artificial Intelligence* 2014; **34**:1 – 12.

[14] An active fault tolerant control approach to an offshore wind turbine model. *Renewable Energy* 2015; **75**:788 – 798.

[15] Fault-tolerant control of wind turbines with hydrostatic transmission using takagi-sugeno and sliding mode techniques. *Annual Reviews in Control* 2015; **40**:82 – 92.

[16] Bianchi FD, De Battista H, Mantz RJ. *Wind turbine control systems*. New York, NY, USA: Springer-Verlag, 2007.

Prepared using acsauth.cls
DOI: 10.1002/acs

[17] Burton T, Sharpe D, Jenkins N, Bossanyi E. *Wind energy handbook*. New York, NY, USA: Wiley, 2008.

[18] Munteanu I, Bratcu AI, Cutululis NA, Caenga E. *Optimal control of wind energy systems - towards a global approach*. New York, NY, USA: Springer-Verlag, 2008.

[19] Merritt HE. *Hydraulic control systems*. John Wiley and Sons, Inc., 1967.

[20] Johnson KE, Pao LY, Balas MJ, Fingersh LJ. Control of variable-speed wind turbines: standard and adaptive techniques for maximizing energy capture. *IEEE Control Systems* 2006; **26**(3):70–81.

[21] Jiang J, Zhang Y. A revisit to block and recursive least Squares for parameter estimation. *Computers and Electrical Engineering* 2004; **30**(5):403–416.

[22] Alessandri A, Baglietto M, Battistelli G. Design of state estimators for uncertain linear systems using quadratic boundedness. *Automatica* 2006; **42**(3):497–502.

[23] Ding B. Constrained robust model predictive control via parameter-dependent dynamic output feedback. *Automatica* 2010; **46**(9):1517–1523.

[24] Ding B. Dynamic output feedback predictive control for nonlinear systems represented by a Takagi–Sugeno model. *Fuzzy Systems, IEEE Transactions on* 2011; **19**(5):831–843.

Prepared using acsauth.cls
DOI: 10.1002/acs